

**DEVELOPMENT OF LIQUID BIOPSY
METHODS FOR LUNG CANCER DETECTION**

SHEFALI SINGH



**DEPARTMENT OF BIOCHEMICAL ENGINEERING
AND BIOTECHNOLOGY**

INDIAN INSTITUTE OF TECHNOLOGY DELHI

MARCH 2023

© Indian Institute of Technology Delhi (IITD), New Delhi, 2023

DEVELOPMENT OF LIQUID BIOPSY METHODS FOR LUNG CANCER DETECTION

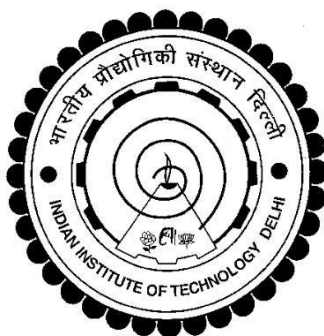
by

SHEFALI SINGH

DEPARTMENT OF BIOCHEMICAL ENGINEERING AND
BIOTECHNOLOGY

Submitted

In fulfillment of the requirements of the degree of Doctor of Philosophy
to the



INDIAN INSTITUTE OF TECHNOLOGY DELHI

MARCH 2023

CERTIFICATE

This is to certify that the thesis titled “**Development of Liquid Biopsy Methods for Lung Cancer Detection**” being submitted by **Ms. Shefali Singh** to the Indian Institute of Technology Delhi for the award of the degree of **Doctor of Philosophy** represents an original and authenticated work performed by her under my supervision and guidance in compliance with the rules and regulations of Indian Institute of Technology Delhi.

To the best of my knowledge, the results embedded in this thesis have not been submitted and will not be submitted in part or full to this institute or any other institute or university for the award of any other degree or diploma.

Date

Prof. Ravikrishnan Elangovan
Associate Professor
Department of Biochemical
Engineering and Biotechnology
Indian Institute of Technology
Delhi
New Delhi - 110016

ACKNOWLEDGMENTS

It gives me immense pleasure to express my gratitude to all who have supported me during this Ph.D. either directly or indirectly. First and foremost, I must thank the almighty for everything that he has bestowed upon me.

I express my profound sense of reverence to Prof. Ravikrishnan Elangovan for his scholastic guidance and moral support. I greatly admire his passion for science and hard-working nature, which has encouraged me and has been one of my biggest motivations throughout my Ph.D. I would like to express heartfelt thanks to him for giving me his valuable time and guidance. His constant guidance and contemporary criticism have given me an opportunity to learn and grow both professionally and personally. I hope to carry forward his enthusiasm in my future endeavours.

I would like to express sincere gratitude to my research committee members: Prof. Ritu Kulshreshtha, Prof. Neetu Singh, and Prof. D. Sundar, for evaluating my work and giving their valuable suggestions for improving it. I am grateful to Dr Prabhat Singh Malik and Dr Sachin Kumar for giving their insights into this work and arranging the necessary resources. I would also like to thank Prof. D. Sundar, Head of the Department, and other faculty members of DBEB for teaching interesting courses and offering support during the last five years.

My special thanks to the Molecular imaging and diagnostics lab members for their help and support during the last five years. My seniors Dr Vikas Pandey, and Dr Vidhu Soman Pillai, for their enriching suggestions and support in managing the lab environment during the conduct of this work. I will always be grateful to them for helping me develop a practical approach to any concept. I can never forget the help and company of my friends- Arti Tyagi, Neha Khaware, Ada Zwetlana, Sneha Kumari, and Neelam Upadhyay who created a healthy environment to work in and motivated me through all the ups and downs during my course of study at IIT-Delhi.

I would further like to show my appreciation to MiMD lab members: Deevanshu Goyal and Dr Raman Karthikeyan for their help with RNA sequencing data analysis and Dr Abhishek Pathak for his support with assay development. Dr Nagarjuna, Dr Gopal, Dr Sampath, and Dr Abhishek for discussing their work experiences and helping me with my submissions.

Thanks, are also due to Bhavika, Jay, Ratnabali, Tushar, and other lab members for maintaining a lively environment in the lab. I am extending my gratitude to Dr Pooja Singh, Dr Saumya Singh, Ms Jyoti Sharma, and Mr Jagat Prajapati for their help during the initial days in the lab.

Special thanks to Mr Prabhu Balasubramanian, Mr Ashutosh Pathak, Mr Ramesh, and Ms Himanshi Singh for managing the lab requirements and their assistance in processing bills.

I am thankful to the DBEB and KSBS lab members for allowing me to use specific instruments. I also thank Prof. Dinda's Nanopath lab in AIIMS-Delhi for providing the necessary instrument support. I would like to thank my department and institute, the Indian Institute of Technology Delhi, for providing me with such a wonderful opportunity to enhance my practical abilities.

I feel blessed and lucky to have the never-ending support of my lifeline, my loving family, at every step of my life: Mom, Dad, and my extremely supportive sister Nidhi and brother Manas. Their continuous love, care, and support have kept me motivated in the pursuit of excellence. My accomplishments are only because of their blessings, and I dedicate this thesis to them.

Date:

Shefali Singh

ABSTRACT

Liquid biopsy (LB) emerged as a new diagnostic concept to address the challenges of cancer diagnosis and therapeutics due to invasive tissue biopsies and clinical imaging. Detection of tumour origin biomolecules such as extracellular vesicles (EVs) and circulating tumour-specific nucleic acids in body fluid samples enables the identification of biomarkers for early cancer diagnosis, prognosis, and theragnostic.

Exosome analysis is a keystone of emerging liquid biopsy techniques, which could serve as a biomarker for early detection. However, the lack of reliable enrichment and detection methods posed a challenge to its clinical utility. In this work, a rapid co-capture-based approach was designed for targeted enrichment and detection of lung cancer-derived exosomes from human plasma. The method involved forming a sandwich complex around the exosomes, which involved magnetic nanoparticles (MNPs) coupled to CD151 to assist in the immunomagnetic selection of lung-derived exosomes and a secondary detection antibody (CD81) coupled to horseradish peroxidase (HRP) for signal amplification. The performance of the co-capture assay to detect exosomes has been optimized with known exosome concentrations and exhibited good linearity ($10^8 - 10^5$ exosomes mL^{-1}) with a detection limit of 60.4 exosomes μL^{-1} . This study further investigated the potential of the developed assay to differentiate healthy and lung cancer patients on clinical samples by quantifying the $\text{CD151}^+/\text{CD81}^+$ lung-derived exosomes.

The method developed for exosome enrichment was further utilized for isolating lung cancer cell-derived exosomes for profiling and identifying the RNA species associated with exosomes to get insights into the altered biology of the disease. Despite the efforts to correctly identify different RNA species and their abundance in EVs, the abundance of RNA species in EVs remains controversial; therefore, unbiased analysis of the exosomal whole transcriptome is necessary. Enriching clinically relevant tissue-specific exosomes may assist in focusing on RNA molecules packaged during cancer. Therefore, the total RNA purified from the enriched fraction of exosomes from patient plasma was characterized using high throughput sequencing. Different RNA biotypes and their differential expression in the exosomes were analysed, and functional enrichment analysis with the list of identified differentially expressed genes (DEGs) found a total of 1383 mRNAs and 64 lncRNA as differentially expressed between patient plasma exosomes than healthy

controls (fold change > 2 , $P < 0.05$). Kyoto Encyclopedia of Genes and Genomes (KEGG) pathway analysis revealed that the DEGs were mainly associated with cancer-related pathways, purine metabolism, calcium, and cGMP-PKG (cyclic-guanosine 3', 5'monophosphate-protein kinase G) signalling pathways.

Circulating Tumour DNA (ctDNA) is emerging as a platform for therapeutic and diagnostic (theragnostic) Tumour monitoring. It provides a non-to-minimally invasive method that is sensitive, specific, and cost-effective for monitoring Tumour growth, relapse, and response to treatment. Therefore, in addition to exploring exosome-based liquid biopsy for early-stage NSCLC screening, we also explored developing a rapid and cost-effective solid-phase extraction-based microfluidic system for cfDNA extraction to deploy it for therapeutic decision guidance.

In conclusion, this study demonstrated a rapid co-capture-based strategy that offers simultaneous isolation and detection of exosomes compatible with low sample volume for detecting lung cancer patients. Further, the exosome enrichment method developed here provided adequate RNA quality for high throughput sequencing. The total transcriptome analysis of lung cancer cell-derived exosomes revealed that the majority of DEGs were involved in cancer-related pathways suggesting that this method could be further utilized to identify disease-specific exosome biomarkers for liquid biopsy-based diagnostic applications. In addition, the successful isolation of cfDNA using the solid phase extraction strategy has been demonstrated for clinical application.

सारांश

इनवेसिव टिशू बायोप्सी और क्लिनिकल इमेजिंग के कारण कैंसर निदान और चिकित्सीय की चुनौतियों का समाधान करने के लिए तरल बायोप्सी (एलबी) एक नई नैदानिक अवधारणा के रूप में उभरी। ट्यूमर मूल बायोमोलेक्यूलस जैसे कि बाह्य पुटिकाओं (ईवीएस) का पता लगाना और शरीर के तरल पदार्थ के नमूनों में ट्यूमर-विशिष्ट न्यूक्लिक एसिड को प्रसारित करना प्रारंभिक कैंसर निदान, रोग का निदान और थेराग्नोस्टिक के लिए बायोमार्कर की पहचान करने में सक्षम बनाता है।

एक्सोसोम विश्लेषण उभरती तरल बायोप्सी तकनीकों का एक कीस्टोन है, जो प्रारंभिक पहचान के लिए बायोमार्कर के रूप में काम कर सकता है। हालांकि, विश्वसनीय संवर्धन और पता लगाने के तरीकों की कमी ने इसकी नैदानिक उपयोगिता के लिए एक चुनौती पेश की। इस काम में, मानव प्लाज्मा से फेफड़ों के कैंसर-व्युत्पन्न एक्सोसोम के लक्षित संवर्धन और पता लगाने के लिए एक तेजी से सह-कैप्चर-आधारित दृष्टिकोण तैयार किया गया था। विधि में एक्सोसोम के चारों ओर एक सैंडविच कॉम्प्लेक्स बनाना शामिल था, जिसमें फेफड़ों से व्युत्पन्न एक्सोसोम के इम्यूनोमैग्नेटिक चयन में सहायता के लिए सीडी 151 के साथ मिलकर चुंबकीय नैनोकणों (एमएनपी) और सिग्नल प्रवर्धन के लिए हॉसरेडिश पेरोक्सीडेस (एचआरपी) के साथ मिलकर एक माध्यमिक पहचान एंटीबॉडी (सीडी 81) शामिल था। एक्सोसोम का पता लगाने के लिए सह-कैप्चर परख के प्रदर्शन को ज्ञात एक्सोसोम सांद्रता के साथ अनुकूलित किया गया है और 60.4 एक्सोसोम μL^{-1} की पहचान सीमा के साथ अच्छी रैखिकता ($10^8 - 10^5$ एक्सोसोम mL^{-1}) का प्रदर्शन किया गया है। इस अध्ययन ने सीडी 151⁺ / सीडी 81⁺ फेफड़ों से व्युत्पन्न एक्सोसोम की मात्रा निर्धारित करके नैदानिक नमूनों पर स्वस्थ और फेफड़ों के कैंसर के रोगियों को अलग करने के लिए विकसित परख की क्षमता की जांच की।

एक्सोसोम संवर्धन के लिए विकसित विधि का उपयोग प्रोफाइलिंग के लिए फेफड़ों के कैंसर सेल-व्युत्पन्न एक्सोसोम को अलग करने और एक्सोसोम से जुड़े आरएनए अणुओं की पहचान करने के लिए किया गया था ताकि रोग के परिवर्तित जीव विज्ञान में अंतर्दृष्टि प्राप्त की जा सके। विभिन्न आरएनए प्रजातियों और ईवी में उनकी बहुतायत को सही ढंग से पहचानने के प्रयासों के बावजूद, ईवी में आरएनए प्रजातियों की बहुतायत विवादास्पद बनी हुई है; इसलिए, एक्सोसोमल पूरे ट्रांसक्रिप्टोम का निष्पक्ष विश्लेषण, आवश्यक है। नैदानिक रूप से प्रासंगिक उतक-विशिष्ट एक्सोसोम को समृद्ध करना कैंसर के दौरान पैक किए गए आरएनए अणुओं पर ध्यान केंद्रित करने में सहायता कर सकता है। इसलिए, रोगी प्लाज्मा से फेफड़ों के कैंसर सेल-व्युत्पन्न एक्सोसोम के समृद्ध अंश से शुद्ध कुल आरएनए को उच्च श्रुपट अनुक्रमण का उपयोग करके विशेषता दी गई थी। एक्सोसोम में विभिन्न आरएनए बायोटाइप्स और उनकी विभेदक अभिव्यक्ति का विश्लेषण किया गया था, और पहचाने गए विभेदक रूप से व्यक्त जीन (डीईजी) की सूची के साथ कार्यात्मक संवर्धन विश्लेषण में कुल 1383 एमआरएनए और 64 एलएनसीआरएनए पाया गया, जैसा कि स्वस्थ नियंत्रणों की तुलना में रोगी प्लाज्मा एक्सोसोम के बीच विभेदक रूप से व्यक्त किया गया था (गुना परिवर्तन > 2 , $P < 0.05$)। जीन और जीनोम के क्योटो विश्वकोश (केईजीजी) मार्ग विश्लेषण से पता चला है कि डीईजी मुख्य रूप से कैंसर से संबंधित मार्गों, प्यूरीन चयापचय, कैल्शियम और सीजीएमपी-पीकेजी (चक्रीय-गुआनोसिन 3', 5'मोनोफॉस्फेट-प्रोटीन किनेज जी) सिग्नलिंग मार्गों से जुड़े थे।

परिसंचारी ट्यूमर डीएनए (सीटीडीएनए) चिकित्सीय और नैदानिक (theragnostic) ट्यूमर की निगरानी के लिए एक मंच के रूप में उभर रहा है। यह एक गैर-से-न्यूनतम इनवेसिव विधि प्रदान करता है जो ट्यूमर के विकास, रिलैप्स और उपचार की प्रतिक्रिया की निगरानी के लिए एक संवेदनशील, विशिष्ट, लागत

प्रभावी तकनीक है। इसलिए, प्रारंभिक चरण एनएससीएलसी स्क्रीनिंग के लिए एक्सोसोम आधारित तरल बायोप्सी की खोज के अलावा, हमने रोगी साइट पर चिकित्सीय निर्णय मार्गदर्शन के लिए इसे तैनात करने के लिए सीएफडीएनए निष्कर्षण के लिए एक तेजी से और लागत प्रभावी ठोस-चरण निष्कर्षण-आधारित माइक्रोफ्लुइडिक सिस्टम विकसित करने का भी पता लगाया।

निष्कर्ष में, इस अध्ययन ने एक तेजी से सह-कैप्चर-आधारित रणनीति का प्रदर्शन किया जो फेफड़ों के कैंसर के रोगियों का पता लगाने के लिए कम नमूना मात्रा के साथ संगत एक्सोसोम के साथ एक साथ अलगाव और पता लगाने की पेशकश करता है। इसके अलावा, यहां विकसित एक्सोसोम संवर्धन विधि ने उच्च श्रूपट अनुक्रमण के लिए पर्याप्त आरएनए गुणवत्ता प्रदान की। फेफड़ों के कैंसर सेल-व्युत्पन्न एक्सोसोम के कुल ट्रांसक्रिप्टोम विश्लेषण से पता चला कि अधिकांश डीईजी कैंसर से संबंधित मार्गों में शामिल थे, यह सुझाव देते हुए कि इस विधि का उपयोग तरल बायोप्सी-आधारित नैदानिक अनुप्रयोगों के लिए रोग-विशिष्ट एक्सोसोम बायोमार्कर की पहचान करने के लिए किया जा सकता है। इसके अलावा, ठोस चरण निष्कर्षण रणनीति का उपयोग करके cfDNA के सफल अलगाव को नैदानिक अनुप्रयोग के लिए प्रदर्शित किया गया है।

CONTENT

CERTIFICATE.....	I
ACKNOWLEDGMENTS	II
ABSTRACT.....	IV
सारांश.....	VI
CONTENT.....	VIII
LIST OF FIGURES	XI
LIST OF TABLES	XVII
ABBREVIATIONS AND SYMBOLS.....	XVIII
Chapter 1: Introduction.....	1
1.1 Exosomes as liquid biopsy marker	1
1.2 Exosome isolation and detection strategies.....	2
1.3 Significance of exosome protein quantification.....	3
1.4 cfDNA-based mutation detection.....	4
Objectives.....	5
Chapter 2: Theory and Background	6
2.1 Lung cancer epidemiology.....	6
2.2 Lung cancer diagnosis and challenges	7
2.3 Therapeutic options for lung cancer	8
2.4 Liquid biopsy.....	11
2.4.1 Circulating Tumour cells	12
2.4.2 Cell-free DNA in plasma	15
2.4.3 Exosomes	24
2.4.4 Tumour-educated platelets (TEPs).....	40
2.5 Liquid biopsy applications	43
2.6 Liquid Biopsy Analysis.....	49
2.6.1 Enzyme Linked Immunosorbent Assay (ELISA)	49
2.6.2 Circulating Nucleic Acid Analysis	50
2.7 Exosomal RNA Analysis.....	58
2.7.1 microRNA (miRNA).....	59
2.7.2 LncRNA	61
2.7.3 mRNA	64

2.7.4	Circular RNA	67
2.8	Research gaps	68
Chapter 3:	Materials and Methods.....	70
3.1	Materials	70
3.2	Exosome Co-Capture Assay	71
3.2.1	Cell Culture Conditioned Media (CCM) Collection	71
3.2.2	CCM Derived Exosome Isolation using Precipitation Method.....	71
3.2.3	MNP-Antibody Conjugation.....	71
3.2.4	Immunomagnetic Capture of A549 Cells and CCM Derived Exosomes.....	72
3.2.5	Collection and Processing of Human Samples	72
3.2.6	Plasma-Derived Exosome Isolation by Precipitation Method	73
3.2.7	Immunomagnetic Capture of Exosomes from Plasma	73
3.2.8	Dynamic Light Scattering (DLS).....	73
3.2.9	Total Exosomal Protein Estimation using Bradford Assay.....	74
3.2.10	High-Resolution TEM (HR-TEM).....	74
3.2.11	Nanoparticle Tracking Analysis (NTA).....	74
3.2.12	Preparation of Calibration Plot for Co-Capture Assay.....	75
3.2.13	Co-Capture of Clinical Samples	75
3.3	Immunomagnetically Enriched Exosome RNA Assessment	75
3.3.1	Exosomal RNA Extraction and Characterization	75
3.3.2	qPCR for Analysis of Exosome-Derived Total RNA	76
3.3.3	cDNA Library Construction and Library Quality Check (QC).....	77
3.3.4	Reads Alignment and Transcriptome Assembly	77
3.3.5	Gene Annotation of Aligned Reads	78
3.3.6	Differential Expression Analysis	79
3.3.7	Functional Enrichment of Differentially Expressed Genes (DEGs)	79
3.4	cfDNA Extraction and Assessment.....	79
3.4.1	cfDNA Extraction from Plasma in Assembled Column	79
3.4.2	Cartridge Design for cfDNA Extraction from Plasma.....	80
3.4.3	Real Time Quantitative PCR Based Quantification of cfDNA.....	82
Chapter 4:	Results and Discussion.....	83
4.1	Exosome Co-Capture Assay	83
4.1.1	Background of the co-capture assay	83

4.1.2	Optimization of MNP-CD151 Based Immunomagnetic Capture Performance	84
4.1.3	Immunomagnetic Enrichment of Cell-Culture Media and Plasma-Derived Exosomes.....	87
4.1.4	Characterization of Enriched Exosomes	88
4.1.5	HRP-CD81 conjugates performance assessment with A549 cells.....	91
4.1.6	Optimization of MNP/HRP Based Co-Capture performance with A549 Cells	93
4.1.7	Optimization of detection conditions for exosomes co-capture.....	95
4.1.8	Preparation of Calibration Curve for Detection of Exosomes	97
4.1.9	Examining the Co-Capture Assay Specificity.....	100
4.1.10	Quantification of Exosomes in Clinical Samples.....	101
4.2	Immunomagnetically Enriched Patient Derived Exosomal RNA Profiling	102
4.2.1	Exosomal RNA Characterization.....	102
4.2.2	Total RNA Sequencing using Illumina Platform	104
4.2.3	Profiling the RNA Packaged Inside the Lung Cancer Cell Derived Exosomes.....	106
4.2.4	Protein Coding RNA Packaged in Lung Derived Exosomes	107
4.2.5	LncRNA packaged in lung cancer derived exosomes.....	116
4.2.6	Functional Enrichment analysis of DEGs identified in lung derived exosomes	124
4.3	cfDNA Extraction and Analysis.....	126
4.3.1	cfDNA Extraction Performance Assessment on Gel	127
4.3.2	cfDNA Extraction Performance Assessment Using qPCR	128
Chapter 5:	Summary and Conclusions	131
	Summary.....	131
	Conclusions.....	135
	Future Work.....	136
	References.....	137
	Appendix	196
	List of Publications	207
	Curriculum Vitae.....	208

LIST OF FIGURES

Figure No.	Title	Page No.
2.1	Distribution of lung cancer cases.	7
2.2	Liquid biopsy overview. This picture depicts the promising sources for a liquid biopsy and the biomolecules that can be studied for possible applications.	12
2.3	Conventional methods for exosome characterization and analysis.	35
2.4	Role of TEPs in assisting cancer spread.	42
3.1	A) Schematic of the sample processing of this study & B) The bioinformatics pipeline that is followed for data analysis of sequenced RNA.	78
3.2	The composition of pretreatment, binding, wash, and elution buffers along with their pH condition utilized for the isolation of cfDNA from plasma samples.	80
3.3	The Lab-on-chip system for the cfDNA extraction. A) Device for automation of extraction process, B) Tabletop sample processing instrument with the assembled cartridges, C) Cartridge design for processing of the clinical samples.	81
4.1	The schematic shows the co-capture assay workflow. It combined immunomagnetic capture with enzymatic signal amplification to detect lung cancer-related exosomes from human plasma. In the assay strategy, both MNP-CD151 and HRP-CD81 conjugates were mixed with clarified plasma to form a sandwich-like structure, as depicted in the inset. It enabled simultaneous capture and detection of immunomagnetically captured lung cancer-associated exosomes based on fluorescence signal generated by the horseradish peroxidase enzyme bound to exosomes.	84
4.2	Immunomagnetic capture of a fixed number of A549 cells mL ⁻¹ with increasing volumes of MNP-Ab conjugates. A) Cells in a randomly selected frame before immunomagnetic capture of A549 cells. B -E) Cells after immunomagnetic capture using different volumes (25, 50, 75, and 100µL) of MNP-Ab conjugates, respectively. F) Cells after immunomagnetic capture using 100 µL of MNP-Ab conjugates at 60X magnification.	85

Figure No.	Title	Page No.
	(Scale bar – 100 μm , 10X magnification)	
4.3	Optimization of immunomagnetic cell capture. A) microscopic images of cells i) before capture, ii) after capture (at 10X magnification), and iii) immunomagnetically captured cells (at 60X magnification). B) change in CCE on varying the ratio of MNP-CD151 conjugate volume to a fixed volume of cell suspension. C) shows an increase in CCE with decreasing cell concentration (10^7 to 10^3 cells mL^{-1}) on using the fixed sample to MNP conjugate ratio (1:20), D) the change in CCE with increasing antibody concentration coupled to MNPs. At higher cell concentrations, the increased antibody amount conjugated to MNPs improved the cell capture efficiency.	86
4.4	Nanoparticle tracking analysis. The difference in the size distribution of A) magnetic nanoparticles, B) immunomagnetically captured cell culture media-derived exosomes, and C) immunomagnetically captured plasma-derived exosomes. An increase in size distribution was observed after the immunomagnetic capture of exosomes.	87
4.5	Dynamic light scattering (DLS) based size assessment of exosomes isolated using two different approaches from CCM and human plasma. An increase in the hydrodynamic size of the MNP-CD151-Exosomes complex is evident after the immunomagnetic capture. Error Bars represent standard deviation, n=14.	88
4.6	Nanoparticle tracking analysis (NTA) measures the size distribution and concentration of the immunomagnetically captured exosomes from cell culture media (CCM) and human plasma.	89
4.7	The transmission electron microscopy (TEM) images of exosomes extracted from A) cell culture media (CCM) using precipitation method, B) cell culture media (CCM) through immunomagnetic capture method, and C) plasma-derived exosomes (PDE) by immunomagnetic capture. The exosomes recovered from both methods were morphologically intact and spherical in shape.	90
4.8	The total exosomal protein concentration obtained from plasma using the precipitation method and immunomagnetic capture approach was estimated and plotted for both methods. Error Bars	91

Figure No.	Title	Page No.
	represent standard deviation, n=7.	
4.9	The schematic workflow for horseradish peroxidase (HRP) based cell detection procedure.	91
4.10	Minimum incubation time required for binding of HRP-CD81 with A549 cells. A selected cell concentration was incubated with HRP-CD81 at three different time intervals (15, 30, and 60) min. Fifteen minutes of incubation with cells was sufficient to provide a significant fluorescence signal increase.	92
4.11	Performance of HRP-CD81 conjugates for lung cancer cell detection. A) Enzyme kinetics of HRP-bound lung cancer cells (A549) at different cell concentrations. B) Based on the fluorescence intensities, linearity ($R^2= 0.995$ was obtained between the detection range of 10^2 to 10^6 cells mL^{-1} . Error bars: standard deviation, n = 3.	93
4.12	MNP and HRP antibody conjugates-based co-capture assessment on A549 cells. Microscopic image of A) A549 cells before immunomagnetic co-capture & after performing co-capture of A549 cells with MNP-CD151/HRP-CD81 conjugates (10x magnification).	93
4.13	Evaluation of co-capture system on A549 cells using MNP and HRP antibody conjugates. An increase in fluorescence intensity was observed compared to different negative controls (background signal) due to the HRP catalysis from the co-captured cells. Error Bars: standard deviation, n=3	94
4.14	MNP/HRP-based co-capture assay performance assessment. A) Enzyme kinetics study of HRP bound to different concentrations of co-captured cells. B) Change in fluorescence intensity observed at different concentrations of immunomagnetically co-captured cells. The calibration curve plotted between fluorescence intensity, and the immunomagnetically co-captured cells presented a good linear detection range between 10^2 to 10^6 cells mL^{-1} . Error bars: standard deviation, n = 3	95
4.15	The enzyme activity of HRP-CD81 conjugates (without exosomes) at different dilutions (1:240 to 1:3840). The increase in fluorescence signal was directly proportional to the HRP concentration in this range.	95

Figure No.	Title	Page No.
4.16	The increase in fluorescence signal after co-capture of a fixed amount of exosomes using four different HRP-CD81 conjugates dilutions (1:1000 to 1:50).	96
4.17	Selection of the working substrate concentration for the exosome co-capture assay. This graph shows the increase in fluorescence signal observed after the co-capture of a fixed amount of exosomes at varying substrate concentrations. The increase in the signal was in proportion to the increasing substrate concentration.	97
4.18	The calibration curve of the co-capture assay for exosome quantification. This graph is plotted between different concentrations of co-captured exosomes and their respective fluorescence intensities, whereas the blue line signifies the baseline fluorescence signal from the negative control, i.e., MNP-CD151/HRP-CD81 conjugates without exosomes. The fluorescence signal increased linearly within 10^5 to 10^8 exosomes mL^{-1} . (Error bar: standard deviation, $n = 4$)	98
4.19	Exosomes co-captured from various cancer and non-cancer cell lines were measured for their relative fluorescence intensity. NIH/3T3 (fibroblast cell line), HT-29 (colorectal carcinoma), LNCaP (prostate cancer), HELA (cervical cancer), A549 cells (lung adenocarcinoma), and L132 (human embryonic lung) were among the examined cell lines. (Error bars: standard deviation, $n = 3$)	100
4.20	Clinical validation of the co-capture assay for distinguishing lung cancer patients from healthy controls. On performing Two sample <i>t-Test</i> , a significantly increased fluorescence signal was observed in the lung cancer population as opposed to non-cancer controls ($P = 0.000332$).	101
4.21	The receiver operator curve (ROC) plotted between clinical sensitivity and specificity to determine the diagnostic power of the exosome co-capture assay for lung cancer detection ($n = 22$).	102
4.22	Characterization of immunomagnetically enriched exosomes and exosomal RNA A) HR-TEM micrograph of exosomes after magnetic capture at 100 nm resolution & the vesicles obtained after capture was morphologically spherical, B) The yield and quality of exosomal RNA obtained from both the exosome isolation methods were compared through qRT-PCR for two	103

Figure No.	Title	Page No.
	mRNA and miRNA targets, (Error Bar = Standard deviation, n=3) C) the total protein concentration of TEI isolated and immunomagnetically captured exosomes was measured & the protein concentration obtained from both methods is shown in the graph for comparison.	
4.23	The total number of genes detected in each sample after sequence alignment.	104
4.24	Protein coding RNA detected in lung cancer cell-derived exosomes: Venn plot showing the total number of protein-coding RNA identified in different categories (control, patients, and common).	107
4.25	Top 50 abundantly packaged exosomal protein-coding RNA in the plasma-derived exosomes based on their FPKM counts.	108
4.26	The overall differentially expressed protein-coding RNA identified based on log ₂ fold change between control and patient-derived exosomes are represented with its statistical significance.	109
4.27	Top 50 DEGs identified between the NSCLC patients and healthy controls using DESeq 2 analysis.	110
4.28	Immunomagnetically enriched exosomal lncRNA profile: Venn diagram represents the total number of lncRNAs detected in different categories (control, patients, and common between both categories).	116
4.29	The box plot depicts the top 20 abundant lncRNAs (based on FPKM counts) packaged in immunomagnetically enriched exosomes derived from clinical samples.	117
4.30	The volcano plot shows the overall DELs (based on log ₂ fold change) identified between patients and healthy controls with its statistical significance.	118
4.31	Immunomagnetically enriched exosomal lncRNA profile. Heat map of top 50 DELs found between patients and healthy controls.	119
4.32	GO enrichment analysis of differentially expressed genes identified in plasma-derived exosomal RNA from lung cancer patients and healthy individuals. The top 10 significant GO terms found between the two groups are represented as A) based on biological processes, B) Based on cellular components, C) based	125

Figure No.	Title	Page No.
	on molecular function & D) The most enriched KEGG pathways.	
4.33	Preparation of calibration plot for assessment of cfDNA recovery. A) Different DNA concentrations (as mentioned above the wells) were loaded directly into each well and run on the 2% agarose gel to generate a calibration plot, B) A calibration graph was plotted between raw integrated density and different DNA concentrations, n=3. n=3.	127
4.34	Evaluation of cfDNA extraction performance using the agarose gel A) The gel image depicting the spiked DNA recovered after extraction through the membrane (the DNA concentrations mentioned above each well are the expected theoretical yield of the recovered DNA loaded in the particular well), B) shows the % recovery after extraction at 100, 500, and 1000 ng spiked DNA concentrations. Error Bars represent the standard deviation, n=3.	128
4.35	Plasma sample pre-processing and liquid operations in the cfDNA cartridge. A) Patient plasma pre-treatment using proteinase K and pre-treatment buffer followed by the addition of binding buffer. B) Liquid operations in cartridge 1) Pre-treated plasma is loaded into sample channel (C1) of the cartridge, 2) Wash buffer 1 is added to Channel 2, and 3) Wash buffer 2 is loaded from Channel 3, 4) Channel 4 was used to load the elution buffer. After completion of all the liquid operations and membrane drying the cfDNA is eluted from the elution chamber.	129
4.36	Detection of GAPDH in cfDNA isolated directly from plasma samples. A) The calibration plot generated between ct values and GAPDH DNA concentrations in the range 5 to 0.00005 ng/ μ L, B) The nucleic acid binding affinity of two membranes, GF/F and GF/B, was evaluated, and while there was no significant difference in performance, GF/F was further used in cartridge assembly for circulating DNA extraction from plasma. C) The performance of in-house buffer for direct cfDNA extraction from clinical samples using in-house assembled column and cartridge was compared and demonstrated. Error Bars represent standard deviation, n=3.	130

LIST OF TABLES

Table No.	Title	Page No.
2.1	A summary of some important US FDA-approved drugs for targeted therapies in lung cancer.	9
2.2	List of currently used technologies for ctDNA detection.	24
2.3	Extracellular vesicles origin and characteristics	26
2.4	A list of exosomal proteins studied for their role in lung cancer	28
2.5	Conventional approaches for exosome isolation.	34
2.6	Summary of merits and demerits of different types of analytical tools for exosomes detection	35
2.7	Record of microfluidic platforms for exosomal isolation and analysis	38
2.8	List of FDA clearance and approvals in the cancer liquid biopsy field for solid tumours.	46
2.9	Different nucleic acid detection methods available for liquid biopsy analysis	51
3.1	Clinical characteristics of the study population for validation of exosome co-capture assay.	72
3.2	Baseline and clinical characteristics of the study cohort	76
4.1	Summarization of previously reported exosome detection methods and their comparative analysis with the developed co-capture assay	99
4.2	Previous reports of EV RNA sequencing employing different library preparation strategies	105
4.3	The role of differentially expressed protein-coding RNA packaged inside the lung-derived exosomes obtained from plasma samples in NSCLC	111
4.4	The role of the top 20 most abundant lncRNA packaged inside the lung-derived exosomes in NSCLC	119
4.5	The role of DE-lncRNA packaged inside the lung-derived exosomes obtained from plasma samples in NSCLC	122

ABBREVIATIONS AND SYMBOLS

mL	Millilitre
GO	Gene ontology
KEGG	Kyoto Encyclopaedia of Genes and Genomes
BSA	Bovine serum albumin
PBS	Phosphate buffer saline
μg	Microgram
μL	Microlitre
DLS	Dynamic light scattering
HR-TEM	High-resolution transmission electron microscopy
NTA	Nanoparticle tracking analysis
AFM	Atomic force microscopy
LB	Liquid Biopsy
LDCT	Low-dose Computed Tomography
PB	Peripheral Blood
FPKM	Fragments Per Kilobase Million
DAVID	Database for Annotation, Visualization, and Integrated Discovery
RT	Room Temperature
NFW	Nuclease free water
cDNA	Complementary DNA
BB	Binding buffer
DELs	Differentially expressed lncRNA
DEGs	Differentially expressed genes
Ab	Antibody
mg	Milligram
NSCLC	Non-small cell lung cancer
EDC	N-(3-Dimethylaminopropyl)-N'-ethyl carbodiimide hydrochloride
NHS	N-Hydroxysuccinimide
MNP	Magnetic nanoparticles
bp	Base pair

°C	degree Celsius
RNA	Ribonucleic Acid
cfDNA	Cell-free DNA
ctDNA	Circulating tumour DNA
miRNA	microRNA
DNA	Deoxyribonucleic acid
LncRNA	Long noncoding RNA
EB	Elution buffer
DMEM	Dulbecco's modified eagle medium
EDTA	Ethylene diamine tetra acetic acid
Fig.	Figure
F12	Ham's F-12 nutrient mix
FBS	Fetal bovine serum
HCl	Hydrochloric acid
HRP	Horseshoe peroxidase
AUR	Amplex Ultra Red
CO ₂	Carbon dioxide
kDa	kilo Dalton
DMSO	Dimethyl sulfoxide
TEI	Total Exosome Isolation Reagent
NCCS	National Centre for Cell Science
min	Minute
mL	Millilitre
mM	Millimolar
ng	Nanogram
CCM	Cell Culture Media
nM	Nanomolar